Mechanism of Enlarged Nonlinear H2 Response of Transverse Modes in RF BAW Devices

RF BAW デバイスにおける横モードの非線形応答増大のメカニズム

Luyan Qiu[1†], Xinyi Li[2,1], Tatsuya Omori[1], and Ken-ya Hashimoto[1]
([1]Chiba University, [2]University of Electronic Science and Technology of China)
邱魯岩 [1†]，李昕熠 [2,1]，大森達也 [1]，橋本研也 [1] ([1] 千葉大学, [2] 電子科技大学)

1. Introduction

Currently, nonlinearity is one of the hottest research topics in RF surface and bulk acoustic wave (SAW/BAW) devices.[1-3]

Yang et al., reported that transverse modes generate relatively strong second harmonics (H2) in RF BAW resonators.[4] The authors' group reported that H2 behavior can be explained well by the first-order perturbation analysis using the *h*-form constitutive relations[5], and it was also shown that H2 including the transverse modes can be explained well by extending the thoery to two dimensional (2D). [6] They also derived an equivalent circuit for nonlinear behaviors based on the 1D perturbation analysis using the *h*-form.[7] The circuit is equivalent to the modified BVD model for linear responses but two voltage sources V_{NT} and V_{NE} are introduced to express generated nonlinear stress and electric field.

This paper discusses extension of the equivalent circuit to include nonlinearity caused by transverse modes in RF BAW resonators, by which the mechanism causing the H2 enlargement at tranverse modes is explored.

2. Analysis procedures

Fig. 1 shows an equivalent circuit for nonlinear analysis of RF BAW resonators proposed in this paper, where multiple acoustic branches are newly added to the circuit given in [7].

The simulation is performed as follows. First step is the linear simulation. Prior to the analysis, all the *LCR* values are determined by fitting using the measured admittance. The peripheral circuits are added to the model, and the total current I_t and acoustic current I_{mn} in the *n*-th branch are estimated. Following to [7], we assume that I_t and I_{mn} are proportional to the electric flux density *D* and stress S_n of the *n*-th mode, respectively.

Next step is the nonlinear simulation. Nonlinear voltages V_{NT} and V_{NE} are calculated by substituting S_n and *D* to the constitutive equations of the *h*-form.

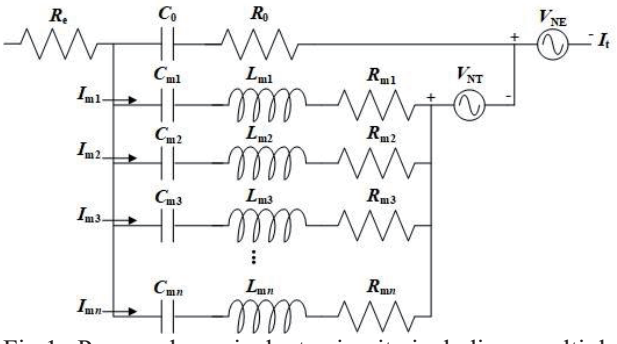

Fig.1 Proposed equivalent circuit including multiple acoustic branches and two signal sources responsible to nonlinear signal generation

The relations are given by

$$V_{NT} = -\sum \beta^S L T_N / h \quad (1)$$

$$V_{NE} = -\sum L E_N \quad (2)$$

$$T_N = -\frac{1}{2}\chi_{20}^T S^2 - \chi_{11}^T SD - \frac{1}{2}\chi_{02}^T D^2 \quad (3)$$

$$E_N = -\frac{1}{2}\chi_{11}^T S^2 - \chi_{02}^T SD - \frac{1}{2}\chi_{02}^E D^2 \quad (4)$$

A weighting factor necessary for the summation over *n* is determined from the motional capacitance C_{mn}. Finally, the peripheral circuits are added again, and H2 output is estimated.

3. Numerical example

As a specimen, we employed a TE mode BAW resonator composed of an AlN piezoelectric layer and two Ru electrodes[8].

Fig. 2 shows the fitted admittance curve of the RF BAW resonator with the measured one. Enlarged view is also given as the inset for frequencies below the main resonance. Series of transverse resonances can be seen at frequenceis lower than the main resonance. The agreement is well not only for the main resonance but transverse modes. In this simulation, 43 resonances were taken into accout.

Fig. 3 compares simulated and experimental H2 of the resonator. In the simulation, only contribution of

†keew@chiba-u.jp

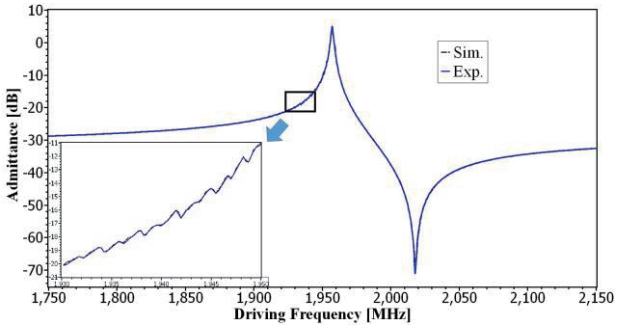

Fig.2 Admittance of the RF BAW resonator

S_1^2 to V_{NT} is considered for the main mode (n=1) while that of $2S_1S_n$ is considered for higher-order modes (n≥2). It is clear from comparison between Figs. 2 and 3 that transverse mode responses are more obvious in H2 than those in the linear response. Good agreement between the simulation and experiment indicates that H2 responses can be simulated accurately and speedy in this manner provided that all the parameters including the weighting factor are known.

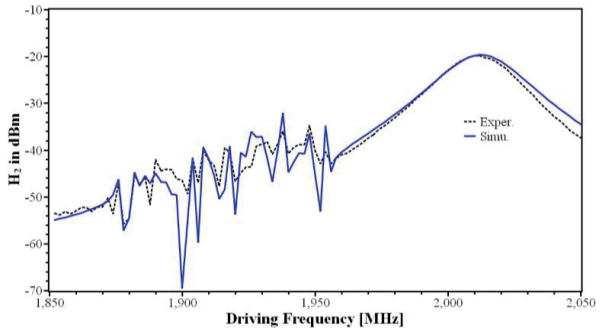

Fig.3 Experimental and simulated H2 responses

4. Discussion

In this case, all the resonance modes included in the simulation are caused by the identical Lamb (S_1) mode. Thus it is expected that all the resonances pocess alsmost identical field distribution toward the thickness direction, and their excitation and detection efficiencies are determined by the resonance field pattern on the electrodes.

Thus it is reasonable to estimate total charge Q_1 induced to the top electrode is given by

$$Q_1 \propto \int_A \left(S_1 + \sum_n S_n \right) dA \qquad (5)$$

for the linear case, where A is the electrode area, and S_n is the lateral field distribution of the n-th resonance. Under the same assumption, total charge Q_n induced as H2 is given by

$$Q_n \propto \int_A \left(S_1 + \sum_n S_n \right)^2 dA \sim \int_A S_1 \left(S_1 + 2\sum_n S_n \right) dA \qquad (6)$$

Note that S_n in Eq. (6) is the same as that in Eq. (5).

For simplicity, S_1 is approximated as uniform (constant) laterally. Then Eqs (5) and (6) reduce to

$$Q_1 \propto S_1 A \left(1 + \frac{1}{S_1 A} \sum_n \int_A S_n dA \right) \qquad (7)$$

and

$$Q_n \propto S_1^2 A \left(1 + \frac{2}{S_1 A} \sum_n \int_A S_n dA \right), \qquad (8)$$

respectively. Comparison of Eqs. (7) and (8) indicates that for higher modes, the detection efficiency for H2 is two times higher than that for the main mode. This fact indicates that H2 of the higher modes is enlarged by a factor of 2 (6 dB) than that of the main one in total. Note that although non-uniform S_1 may cause deviation of this factor from two, the deviation does not seems to be so large.

4. Conclusion

This paper discussed the mechanism causing the H2 enlargement of transverse mode resonances, and it is shown that a factor of 2 appearing at the production of two field components is responsible to this phenomenon.

Acknowledgement

The authors thank Dr. M.Ueda and Mr. T.Nishihara of Taiyo Yuden, Co. Ltd. for their fruitful discussions and supplying the measured data. L.Qiu acknowledges financial support from Frontier Science Program of Graduate School of Science and Engineering.

References

1. K.Hashimoto, et al., Proc. 2017 NOLTA, 2017, p. 193
2. D.Feld, et al., Proc. IEEE Ultrason Symp (2009) pp. 1082-1087
3. D.S.Shim, et al., International Journal of RF and Microwave Computer-Aided Engineering, **21** (2011) p. 486
4. T.Yang, et al., Proc. IEEE Ultrason. Symp (2017) 10.1109/ULTSYM.2017.8092136
5. K.Hashimoto, et al, Proc. European Time and Frequency Forum (2017) pp.538-541
6. L.Qiu, et al., Jpn. J. Appl. Phys., **58**, 7 (2019) SGGC02
7. K.Hashimoto, et al., Proc. IEEE Ultrason. Symp. (2019) [to be published]
8. S.Taniguchi, et al., Proc. IEEE Ultrason. Symp. (2007) pp. 600-603